NeuroImage 316 (2025) 121310

Contents lists available at ScienceDirect

NeuroImage

journal homepage: www.elsevier.com/locate/ynimg

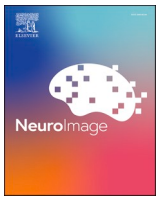

Somatosensory cortical representations of the assimilation effect for vibrotactile stimulation

Ji-Hyun Kim [a], Dooyoung Jung [a], Junsuk Kim [b,**], Sung-Phil Kim [a,*]

[a] Department of Biomedical Engineering, Ulsan National Institute of Science and Technology, Ulsan, South Korea
[b] School of Information Convergence, Kwangwoon University, Seoul, South Korea

ARTICLE INFO

Keywords:
Vibrotactile
Somatosensory cortex
fMRI
Assimilation effect
Connectivity

ABSTRACT

Specific sensory pathways are well-described, but relatively less is known about how these different sensory information streams are integrated to create a coherent representation of the external environment. Several sensory illusions can help reveal these integration mechanisms. This study investigated the neural activity patterns associated with the assimilation effect in the perception of vibrotactile stimuli. The assimilation effect refers to a tactile perceptual bias in which the vibrotactile frequency perception on one finger is biased toward the frequency of a distracting vibrotactile stimulus on a different finger. The assimilation effects occur not only between fingers of the same hand (across-finger) but also between fingers on different hands (across-hand). These behavioral aspects of the assimilation effect led to the assumption that neural processes related to the assimilation effect would involve integrating different tactile information mediated by the somatosensory cortex. We addressed this hypothesis by investigating brain responses using functional magnetic resonance imaging (fMRI) to vibrotactile stimuli that induced the assimilation effect under across-finger and across-hand conditions. As expected, vibrotactile stimuli activated the primary (S1) and secondary (S2) somatosensory cortices. However, these local neural responses did not correlate with the assimilation effect among individuals. Instead, the connectivity between S1 and medial prefrontal cortex (mPFC) was correlated with individual across-finger assimilation effects and connectivity between S2 and inferior parietal lobule (IPL) with individual across-hand assimilation effects. These results suggest that the assimilation effect may be related to tactile information integration via functional connections between the somatosensory cortex and higher-order brain regions.

1. Introduction

The somatosensory system processes tactile information from various mechanoreceptors distributed throughout the body (Abraira and Ginty, 2013; Johansson and Flanagan, 2009). Different types of tactile stimuli are transduced and transmitted by distinct tactile afferents connected to cutaneous receptors (Johnson, 2001), broadly classified as rapidly adapting (RA) and slowly adapting (SA) (Johansson and Vallbo, 1983). Non-human primate studies have shown that neural signals transmitted by RA and SA afferents arrive at distinct columns and layers of area 3b in the primary somatosensory cortex (S1) (Mountcastle et al., 1969; Sur et al., 1984) and that S1 neurons receiving either SA or RA afferent inputs form distinct clusters (Chen et al., 2001; Friedman et al., 2004).

Although it remains unknown how S1 neurons in humans are distributed according to SA and RA afferent inputs, findings in human behavioral studies have indicated that different types of tactile stimuli are also perceived separately. A study reported that adaptation to flutter, which predominantly causes the desensitization of RA type I (RA-I) and SA type I (SA-I) afferents, did not affect the fine-texture discrimination mediated by RA type II (RA-II) afferents (Bensmaïa and Hollins, 2005). This finding suggests that the human somatosensory cortex may also represent different types of tactile stimuli in a segregated fashion.

Although different types and locations of tactile stimuli are perceived independently, the brain integrates them to form coherent tactile perception, such as texture recognition (Rostamian et al., 2022). One of those perceptual phenomena is a biased perception known as the assimilation effect (Sherif et al., 1958). A behavioral study demonstrated

* Corresponding author at: Department of Biomedical Engineering, Ulsan National Institute of Science and Technology, 50 Unist-gil, Eonyang-eup, Ulsan, 44191, South Korea
** Corresponding author at: School of Information Convergence, Kwangwoon University, 20 Kwangwoon-ro, Nowon-gu, Seoul, 01897, South Korea
E-mail addresses: junsuk.kim@kw.ac.kr (J. Kim), spkim@unist.ac.kr (S.-P. Kim).

https://doi.org/10.1016/j.neuroimage.2025.121310
Received 25 February 2025; Received in revised form 2 June 2025; Accepted 5 June 2025
Available online 6 June 2025

the assimilation effect in vibrotactile perception (Kuroki et al., 2017). Subjects judged the frequency of a target (30 Hz) vibrotactile stimulus to a finger while simultaneously receiving a distractor vibrotactile stimulus at a much different frequency (240 Hz) to either an adjacent finger on the same hand (across-finger condition) or to the same finger on the opposite hand (across-hand condition). The large frequency difference was intended to engage different mechanoreceptor channels, enabling investigation of vibrotactile integration. The results showed that subjects' judgments of the target frequency were systematically biased toward the distractor frequency under both the across-finger and across-hand conditions. This effect was observed even when the target and distractor stimulus frequencies were reversed. Even when stimuli were applied to distinct somatotopic regions, the distractor still influenced target perception, suggesting cortical-level integration. However, the neural correlates of the assimilation effect on tactile perception remain unclear.

Therefore, we used functional magnetic resonance imaging (fMRI) to examine the neural basis of the vibrotactile assimilation effect. Previous studies on tactile illusions have also shown responses in both specific regions related to the stimulated body part (a somatotopic region in S1) and non-specific regions. In a primate study on the tactile funneling illusion, optical imaging revealed distinct S1 responses to unilateral illusory stimulation (Chen et al., 2003). In an fMRI study on the Cutaneous Rabbit illusion in which stimulation was applied to one forearm, significant blood oxygenation level-dependent (BOLD) responses were observed in the premotor and prefrontal cortex during the illusory condition (Blankenburg et al., 2006). Another study on the velvet illusion involving stimulation of both hands revealed significantly stronger connectivity between S1, secondary somatosensory cortex (S2), and the superior parietal lobule during the illusory condition (Rajaei et al., 2018).

Studies of other sensory modalities further suggest the involvement of brain regions in assimilation effects. In human experiments using visual luminance stimuli and electroencephalographic (EEG) measures of event related potentials, distinct signals for contrast and assimilation were observed at occipital and parietal sites during the early N1 time window, implicating the parietal cortex in the assimilation effect (Acaster et al., 2021). Additionally, a neuroimaging study reported that neural responses in the S2 were increased among subjects exhibiting an assimilation effect while perceiving flavor stimuli (Davidenko et al., 2018). Therefore, S2 activity may contribute to tactile assimilation, even when assimilation is induced by a different sensory modality.

To investigate the neural correlates of vibrotactile assimilation, we adopted the behavioral paradigm of Kuroki et al. (2017). During fMRI scanning, subjects discriminated the supra-threshold vibrotactile stimulus frequencies of a target (30 Hz) while simultaneously receiving a higher-frequency distractor (200 Hz) on an across finger within the same hand or across hands. A control condition used a distractor with the same frequency as the target, and a test condition used a distractor with a much higher frequency to probe the assimilation effect. The assimilation effect is identified by comparing the test with the control condition.

We hypothesized that presenting vibrotactile stimuli of different frequencies at distinct somatotopic locations would alter the perceived frequency and increase BOLD responses in somatosensory regions. In a previous study, vibrotactile stimulation induced responses across all S1 subregions (BA 3, 1, 2) when delivered to individual fingers (Schellekens et al., 2021). Based on these findings, if integration of stimuli across different fingers occurs within S1, BA2 is expected to have the greatest influence, leading to stronger BOLD responses in S1 due to its broadest receptive fields among the subregions. In addition to S1, S2 has broad receptive fields and is involved in higher-order processing of tactile information relayed from S1 and the thalamus (Eickhoff et al., 2007). Therefore, S2 may integrate different types of tactile signals, which could lead to interference between signals and result in increased BOLD activity.

While broad receptive fields and high-frequency responsiveness may support local integration, the assimilation effect likely involves broader network interactions. Therefore, the assimilation effect may alter the functional connectivity between the somatosensory cortex and higher-order brain regions, such as the parietal and prefrontal cortices, which are implicated in advanced tactile processing, including tactile discrimination (Hartmann et al., 2008) and tactile illusion (Rajaei et al., 2018). Moreover, to ensure that neural activity patterns are actually involved in perceptual assimilation rather than merely representing responses to high-frequency stimuli with wider receptive fields, we conducted a correlation analysis between neural activity measurements and individual variations in the magnitude of the assimilation. This correlation analysis provided stronger evidence for a relationship between the neuronal responses and the assimilation effect.

2. Materials and methods

2.1. Subjects

Thirty-nine subjects (20 females; mean age 25.4 years old; age range 19-35 years old) with no contraindications against MRI and no history of neurological disorders participated in this study. Only right-handed subjects were recruited to control for the handedness effect. Each subject participated in the pre-experiment and behavioral experiment. Seven subjects whose behavioral data could not be fitted by a general psychometric curve for tactile frequency perception were excluded during the processing of behavioral data (see Section 2.6. *Behavioral data analysis*). Therefore, only 32 subjects participated in the fMRI experiment. After scanning, three subjects were also excluded due to the absence of distinguishable regions of interest (ROI) (see Section 2.9. *Determination of the local ROIs*). Consequently, the data of 29 subjects were used in the main analyses. This study was approved by the ethics committee of the Ulsan National Institute of Science and Technology (UNISTIRB-21-54-C). All methods were followed relevant institutional guidelines and regulations. All subjects were informed of the study objectives and experimental procedures and voluntarily submitted a written consent form.

2.2. Vibrotactile stimuli

This study adopted the vibrotactile stimulus regimens from a previous report demonstrating the assimilation effect on tactile perception (Kuroki et al., 2017). Two primary frequencies were used: 1) a target frequency of 30 Hz; and 2) a distractor frequency of 200 Hz. A 200-Hz distractor was applied rather than the 240-Hz distractor as in Kuroki et al. (2017) because the piezoelectric tactile stimulator (PTS) used in the current study elicited a resonance effect for stimuli over 200 Hz, significantly reducing the stimulus amplitude. Nonetheless, a vibrotactile frequency of 200 Hz is sufficiently high to stimulate RA-II receptors (Dykes et al., 1981). Then, we set the frequency of six comparison vibrotactile stimuli around the target frequency (15, 21, 25, 36, 42, and 60 Hz) to assess frequency discrimination. These same frequencies were used by Kuroki et al. (2017). All vibrotactile stimuli were synthesized as the sinusoidal signals using MATLAB 2019b (Mathworks, Inc., Natick, MA, USA). In addition, Tukey windowing was used to reduce the prominence of skin deformation on the onset and offset of stimulation (Kuroki et al., 2017). All vibrotactile stimuli were delivered using three 6-mm diameter MRI-compatible PTS devices (Dancerdesign, St. Helens, UK) attached to the middle and index fingertips of the left hand and to the index fingertip of the right hand. The amplitude of the target stimulus (30 Hz) was fixed at 0.4 arbitrary units (AU). Then, the distractor and comparison stimulus amplitudes were adaptively determined for each subject during a pre-experiment.

2.3. Pre-experiment for perceptual matching

The pre-experiment was designed to balance the perceived intensities of all vibrotactile stimuli for each subject. This procedure was required because the PTS devices used in this study delivered greater amplitude stimuli as the frequency increased. In addition, it is known that the perceived vibrotactile intensity varies with the frequency (Prsa et al., 2021). Therefore, we aimed to ensure that each subject perceived the same intensity for all the vibrotactile stimuli by adjusting the amplitude of each stimulus individually. To set the initial amplitude of each stimulus, we utilized a dataset generated by our laboratory in a different study where 57 subjects performed the same task to discriminate the same vibrotactile stimuli provided by the same devices used in the current study (Jeong et al., 2022). We applied the staircase method to determine the amplitude of each stimulus so that the perceived intensity of every stimulus was equalized in each subject (Wetherill and Levitt, 1965). We employed both the 3-up/1-down (ascending) and 3-down/1-up (descending) staircase algorithms. A reversal was defined as a change in the direction of the staircase (from ascending to descending or vice versa). The staircase procedure ceased after six reversals. The mean amplitude was obtained by taking the average of the six reversal points. Then, the final amplitude was determined by averaging the mean amplitudes obtained from both the ascending and descending staircase algorithms. The average amplitudes across all 57 subjects were then used as initial values for the current study (Fig. 1).

In the pre-experiment, subjects sat on a chair with both hands extended forward and palms facing down, and were instructed to gaze at a monitor initially displaying a black cross on a gray background. Trial onset was cued by a change from the black cross to a white cross, after which a pair of vibrotactile stimuli were delivered simultaneously to the index and middle fingers of the left hand for 1 s. One of the pair was the target stimulus (30 Hz) with a fixed amplitude (0.4 AU) and other was either one of the comparison stimuli (15, 21, 25, 36, 42, and 60 Hz) or the distractor stimulus (200 Hz) with an adaptive amplitude (Fig. 2A and B). The finger stimulated by the target stimulus and that stimulated by the comparison or distractor stimulus (index or middle) were fully randomized. After the 1-s stimulation period, the word “response” was displayed on the screen, and the subjects were requested to indicate which stimulus intensity was higher using a foot pad. Subjects pressed a left foot pad if the stimulus to the middle finger felt stronger and the right foot pad if the stimulus to the index finger felt stronger. The trial ended with the subjects’ response, and a subsequent trial began after a 2-s inter-trial interval. First, we presented a stimulus pair for 30 trials in a single run for each of the six comparison stimuli and one distractor stimulus, using averaged amplitudes derived from 57 subjects in the previous experiments (Fig. 1). We assumed that if more than two-thirds of the trials were biased towards one choice, the perception of the current comparison stimulus amplitude would not match that of the target stimulus amplitude. If subjects rated one of the stimuli as stronger in more than 19 trials, we deemed the perceived intensities of the two stimuli as mismatched. After confirming the mismatch, we adjusted the amplitudes of the comparison and distractor stimulus using the 3-up/1-down and 3-down/1-up staircase methods (Wetherill and Levitt, 1965). We repeated these runs until the perceived intensities of the two stimuli were matched. In no case was the staircase procedure performed more than once across all subjects. For each subject, the total number of trials could range from 210 if each of the 7 stimuli were presented for 30 trials without adjustment via the staircase procedure, to 420 if all 7 stimuli were presented for 60 trials, with 30 trials conducted both before and after adjustment. The current experiment performed this matching confirmation task for 260.91±45.30 trials on average.

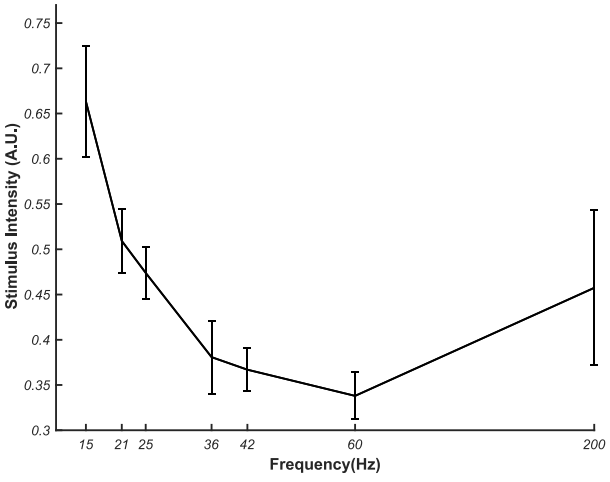

Fig. 1. Mean adjusted amplitudes of the vibrotactile stimuli used in the current study. The amplitudes of the non-target stimuli were adjusted using the 3-up/1-down and 3-down/1-up algorithms based on subject responses to match perceptual intensity with that of the target stimulus (30 Hz, set to an intensity of 0.4 AU). The error bars denote the standard error of the mean across subjects who participated in the other study of amplitude equalization across stimulus frequencies ($N = 57$).

2.4. Behavioral experiment

The subjects performed the behavioral tactile discrimination task in the same room after the pre-experiment. The break time between the pre- and behavioral experiment was less than 5 min. We adopted the behavioral experimental paradigm described in the previous study (Kuroki et al., 2017). The behavioral experiment included three main conditions differing according to vibrotactile stimulus type and location: Non-Distractor (ND), Across-Finger (AF), and Across-Hand (AH) conditions. In all conditions, the same sequence was employed: 1) a target period with the presentation of the target stimulus (30 Hz for 1 s) with or without the distractor; 2) interstimulus interval (1 s); and 3) a comparison period with the presentation of one of the comparison stimuli (1 s).

In the ND condition, the target stimulus was delivered to a target finger (index or middle) of the left hand without the distractor stimulus. The target finger was counterbalanced across subjects. Also, within each subject, the target finger remained consistent across all blocks. In the AF condition, the left index or middle finger, different from the target finger (termed the distractor finger), was simultaneously stimulated during the target period. The AF condition was further divided into two subconditions in which both target stimulus and distractor stimulus frequencies were 30 Hz (the AF control condition, AFc) or the distractor stimulus was 200 Hz (the AF test condition, AFt) (Fig. 2C). The AH condition was the same as the AF condition, except that the target and distractor stimuli were delivered to the index fingers of opposite hands. We assumed that the simultaneously presented distractor would induce assimilation, and so expected the assimilation effect to be more pronounced in the test condition. We compared the ND, control, and test conditions across the AF and AH configurations to assess the presence of assimilation. Each trial consisted of vibrotactile stimulations over three periods as described above, as well as the behavioral responses. A trial was conducted in blocks defined by finger stimulation configuration and task condition. The locations of the target and distractor fingers were alternated in two different finger arrangements for each condition. At the beginning of a block, a text instructing the subject to pay attention to the stimulation on the target finger appeared on the screen. Afterward, a black fixation cross appeared on the screen for 1 s and turned to white to cue the start of the stimulus presentation. The cross became white only during stimulation and remained black otherwise. After the comparison period, the subjects responded which of the target and comparison stimulus vibrated at a higher frequency. Subjects pressed the left foot pad if the frequency of the target stimulus was perceived higher, and the right foot pad if the comparison stimulus frequency was perceived as

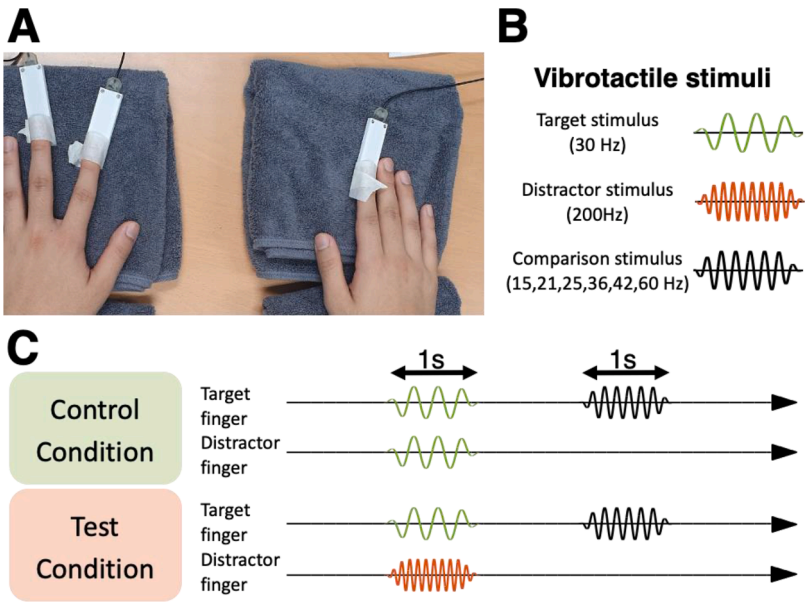

Fig. 2. Experimental setup and stimuli used to induce and evaluate the assimilation effect. (A) Attachment of stimulators to the fingers for all experimental conditions. The three stimulators were attached to the left middle fingertip, left index fingertip, and right index fingertip with palms facing down, resting on a towel. (B) Vibrotactile stimuli used in the study are divided into three types: target stimulus at 30 Hz, distractor stimulus at 200 Hz, and comparison stimuli at 15, 21, 25, 35, 42, and 60 Hz for testing frequency discrimination. (C) The conditions of stimulus presentation. Under the control condition, the 30-Hz target stimulus was delivered to both the target and distractor fingers simultaneously for 1 s. After a 1 s inter-stimulus interval, one of the comparison stimuli was delivered to the target finger for 1 s. Under the test condition, the target stimulus was delivered to the target finger, and the 200-Hz distractor stimulus was delivered to the distractor finger at the same time for 1 s. After a 1 s inter-stimulus interval, one of the comparison stimuli is delivered to the target finger for 1 s.

higher.

Each of the six comparison stimuli was presented 10 times in a random order within a block, so that every block consisted of 60 trials. The subjects performed a total of 10 blocks (600 trials) with 2 blocks under the ND condition (either the left index or middle finger was the target in each block), 4 blocks under the AF condition (the left index finger was the target finger in 2 blocks and the left middle finger was the target finger in the other 2 blocks), and 4 blocks under the AH condition (again, the left index finger was the target finger in 2 blocks and the right index finger was the target finger in the other 2 blocks) (Fig. 3A). In a single block under the AF or AH configuration, the control (AFc or AHc) and test (AFt or AHt) conditions were presented in a pseudorandom

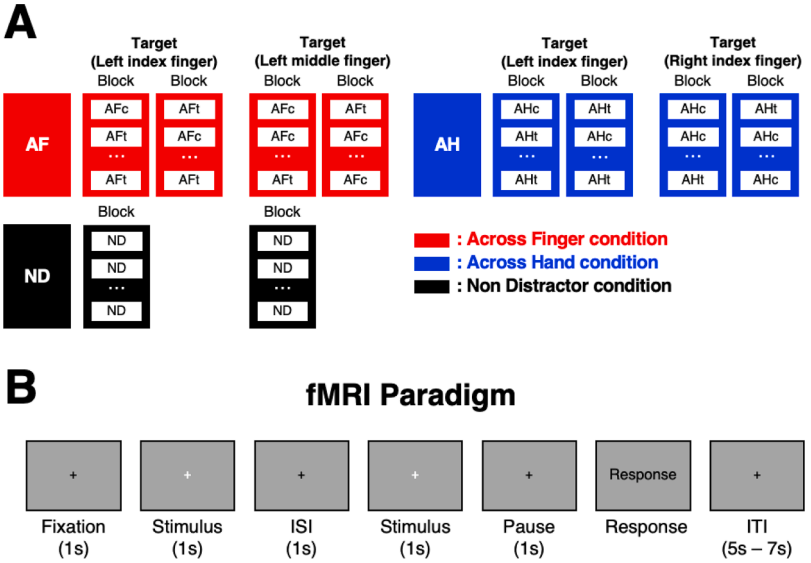

Fig. 3. Experimental paradigm. (A) Conditions of the behavioral task. Subjects performed the behavioral task where they had to discriminate the higher frequency of the two stimuli (target and comparison stimuli) in each of the three conditions: across-finger (AF), across-hand (AH), and non-distractor (ND). In the AF and AH conditions, stimuli were presented in either the control condition (AFc, AHc) or the test condition (AFt, AHt) for each trial. The control and test conditions were randomly presented in a block of the behavioral condition. Each block contains 30 trials of the control and 30 trials of the test conditions. Two blocks were included for each finger configuration (the left index finger as the target or left middle finger as the target in the AF condition and the left index finger as the target or right index finger as the target in the AH condition). There was no-distractor stimulus in the ND condition. (B) Experimental design for the fMRI experiment. A white cross appears at the center of the screen when stimuli were presented. The subjects had to discriminate the higher frequency of the two stimuli when the word "response" was displayed. An inter-trial interval varied randomly between 5 s and 7 s.

order to balance the number of presentations between the comparison stimuli. The order of the ND, AF, and AH blocks was fully randomized.

2.5. Functional magnetic resonance image experiment

The fMRI experiment was conducted 2.15 ± 1.29 days on average after the behavioral experiment. Three PTS devices were attached to the fingers in the same way as in the behavioral experiment, while subjects' palms facing down. To ensure no effect of finger movements on tactile perception, we instructed the subjects to refrain from moving their fingers throughout the experiment. Additionally, we positioned the subjects' hands in a manner to minimize discomfort. Visual monitoring was conducted to ensure adherence to these instructions, and revealed no significant movements. The fMRI experimental paradigm was identical to the behavioral experimental paradigm except that each comparison stimulus was presented four times (instead of ten) per block due to the time limitations of MR scanning. During fMRI experiment, the subjects perceived stimuli and pressed an MRI-compatible foot pad through the flexion and extension of their toes, similar to the behavioral experiment (Fig. 3A). Pressing the foot pad sent a trigger signal to the computer to control the experimental paradigm for synchronization, which allowed for recording the precise onset of the subject's response. Also, an inter-trial interval was set to 5 to 7 s to meet the requirement for the hemodynamic response function (HRF) to return to baseline (Fig. 3B).

2.6. Behavioral data analysis

We estimated the psychometric function for behavioral responses in the perceptual discrimination of vibrotactile frequency using the Palamedes toolbox 1.10.11 running in MATLAB (Prins et al., 2018). The behavioral data collected from both the behavioral and fMRI experiment were aggregated and used for this estimation. Paired t-test results showed that the point of subject equality (PSE) values derived from the behavioral experiment outside the MRI scanner were not significantly different from those obtained during fMRI experiment, for any condition (ND: $t(28) = 0.972$, $p = 0.339$; AFc: $t(28) = 0.700$, $p = 0.490$; AFt: $t(28) = -1.954$, $p = 0.061$; AHc: $t(28) = -0.072$, $p = 0.943$; AHt: $t(28) = -1.503$, $p = 0.144$). This statistical analysis result does not invalidate our approach of combining the data from both behavioral and fMRI experiment to estimate individual PSE values. In total, 28 trials were recorded for each ND, AFc, AFt, AHc, and AHt condition, 20 conducted outside the fMRI scanner and 8 during fMRI. For each comparison stimulus under each condition in each subject, we calculated the ratio of the number of trials where the comparison stimulus frequency was perceived as higher than the target stimulus frequency to the total number of trials for that comparison stimulus. A logistic function was used as the psychometric function and fitted to the calculated ratio of each comparison stimulus under each condition in each subject. The Nelder-Mead simple search algorithm was used to maximize the likelihood of the psychometric function (Nelder and Mead, 1965). Subjects were considered to have an abnormal psychometric function if they never responded that comparison stimuli were of a higher frequency than the target stimulus or showed a decreasing trend in their responses as the comparison frequency increased. Seven subjects whose psychometric curves could not be fitted to their behavioral responses did not proceed to the fMRI experiment.

From the psychometric functions for each subject, we calculated the PSE, defined as the estimated frequency of the comparison stimuli corresponding to 50 % of the ratio on the fitted psychometric curve. A previous behavioral study revealed that the assimilation effect can be indicated by the PSE difference between the test and control conditions (Kuroki et al., 2017). We verified that for all conditions, PSE values showed no evidence supporting the violation of normality as assessed by the Kolmogorov-Smirnov normality test (ND: $p = 0.694$, AFc: $p = 0.134$, AFt: $p = 0.676$, AHc: $p = 0.564$, AHt: $p = 0.918$). The significance of the PSE difference between ND, AFc, and AFt conditions as well as between ND, AHc and AHt conditions was statistically evaluated using the one-way repeated measures ANOVA (rmANOVA) test ($\alpha = 0.05$), followed by Tukey's post-hoc test for multiple pairwise comparisons. Through this statistical analysis, we tested the null hypothesis that the PSE values were identical across all conditions.

2.7. MRI data acquisition and preprocessing

The MRI scanning was conducted using a 3 T scanner (Magnetom TrioTim, Siemens, Germany) equipped with a 64-channel head coil at the Center for Neuroscience Imaging Research in Suwon, Republic of Korea. Three-dimensional (3D) functional images were acquired using a slice-accelerated multiband gradient-echo-based echo planar imaging (EPI) sequence with T2*-weighted BOLD contrast covering the whole brain region (multiband acceleration factor = 2, number of slices = 72, repetition time (TR) = 2,000 ms, echo time (TE) = 35 ms, flip angle = 90°, field of view (FOV) = 200 mm, slice thickness = 2 mm and voxel size = 2.0 × 2.0 × 2.0 mm^3). In addition, anatomical high-resolution images were obtained using a T1-weighted 3D MPRAGE sequence with the following parameters: TR = 2,300 ms, TE = 2.28 ms, flip angle = 8°, FOV = 256 mm, and voxel size = 1.0 × 1.0 × 1.0 mm^3). The functional images were preprocessed using SPM12 software (Wellcome Department of Imaging Neuroscience; London, UK). Preprocessing steps for functional images included slice-timing correction, realignment, co-registration, segmentation, spatial normalization to the Montreal Neurological Institute (MNI) template, and smoothing with a 6-mm full-width-at-half-maximum isotropic Gaussian kernel.

2.8. Univariate analysis of the fMRI data

Preprocessed fMRI data were analyzed using the general linear model (GLM) to identify individual voxels activated by the vibrotactile stimulation. The BOLD responses of single voxels were modeled using the SPM canonical HRF. Regressors of the design matrix in the GLM analysis within a single block included the following: 1) the onset of the target period under the control condition; 2) the onset of the target period under the test condition; 3) the onset of the comparison period regardless of the condition; and 4) the onset of the subjects' responses. Additional regressors of no interest for motion correction parameters and a linear scanner drift were included in the design matrix. We created a contrast of beta estimates for the stimulus condition to determine the voxels activated by the vibrotactile stimuli. Then, the group-level analysis was conducted with a one-sample t-test using the contrast images obtained from the contrast analysis above. The resulting contrast maps were thresholded to correct for multiple comparisons using cluster-level inference (Woo et al., 2014). We used a significance threshold of $p < 0.05$ family-wise error (FWE) for multiple comparisons correction at the cluster level and a height threshold of $p < 0.001$ at the voxel level.

2.9. Determination of the local ROIs

After obtaining the contrast maps, we determined the local ROIs in each subject for each of the AF and AH conditions by assuming that each subject would have a different peak activation location even in the same anatomical region. The ROIs were determined based on the following criteria. First, we restricted the ROIs to the somatosensory cortex because the primary aim of the study was to identify neural correlates of the assimilation effect within this region. Specifically, among all the clusters of activated voxels identified by the second-level analysis of stimuli vs baseline, we focused on those clusters that exhibited peak responses within the postcentral gyrus (corresponding to S1) or the Rolandic operculum (corresponding to S2). These two regions were defined using the Automated Anatomical Labeling 3 (AAL3) (Rolls et al., 2020). Second, we sought individual peak activation locations within a

volume with a 12-mm diameter centered at the local maximum determined by the group-level analysis (McLaren et al., 2012). Third, an ROI for each subject was determined as a set of voxels that showed the same contrast (stimuli vs. baseline, threshold of $p < 0.05$, uncorrected) and were located within an 8-mm distance from the individual peak activation location (Yu et al., 2018). Note that we used stimuli vs baseline contrast to determine ROIs as we aimed to find local somatosensory cortical regions involved in processing a set of tactile stimuli presented in this study. All ROIs of S1 were included in the regions identified by the previous meta-analysis (Holmes and Tamè, 2019). All ROIs of S1 and S2 were included in the regions identified by another previous meta-analysis (Yarkoni et al., 2011). We excluded the data of three subjects from the analyses using ROIs because no ROIs satisfying the selection criteria were found.

2.10. Percent signal change analysis of fMRI data

We first analyzed the relationship between local regional activity and the behavioral outcomes of the assimilation effect. We investigated whether the percent signal change (PSC) in individual local ROIs of the somatosensory cortex was related to individual PSE values. Through this analysis, we aimed to test the null hypothesis that local PSC within the somatosensory cortex remains constant across conditions, as well as the null hypothesis that individual differences in local PSC are unrelated to variations in PSE. We applied the Marsbar toolbox (Brett et al., 2002) to determine the PSC in each specified ROI for each condition—AFt, AFc, AHt, and AHc. To compute the PSC, we first multiplied the beta weight by the highest value of the regressors for individual trials for each condition. We divided this product by the beta weight for the constant regressor, which served as a baseline measurement. Next, we examined the effects of each ROI and each condition on the PSC. None of the group PSC data were found to deviate significantly from normal distribution according to the Kolmogorov-Smirnov normality test (right S1-AFt: $p = 0.412$; right S1-AFc: $p = 0.151$; left S2-AFt: $p = 0.145$; left S2-AFc: $p = 0.098$; right S2-AFt: $p = 0.066$; right S2-AFc: $p = 0.473$; left S1-AHt: $p = 0.077$; left S1-AHc: $p = 0.072$; right S1-AHt: $p = 0.075$; right S1-AHc: $p = 0.237$; left S2-AHt: $p = 0.365$; left S2-AHc: $p = 0.081$; right S2-AHt: $p = 0.193$; right S2-AHc: $p = 0.180$). A two-way rmANOVA was used to test the main effects of conditions (independent variable 1) and regions (independent variable 2), followed by Tukey's post-hoc test for multiple comparisons. Differences in the PSC between the test and control conditions do not necessarily support the conclusion that the corresponding neural responses represent the assimilation effect because those differences could simply reflect differential neural responses to multiple tactile stimuli compared to a single stimulus. Thus, we further investigated whether the PSC differences were correlated with the degree of behavioral change by the assimilation effect. To this end, we calculated the Pearson correlation coefficient between the PSC difference and the PSE difference across individual subjects for each ROI, where the PSE difference was measured between the test and control conditions.

2.11. Brain connectivity analysis of fMRI data

We analyzed whether the assimilation effect involved inter-regional connectivity beyond local activation in S1 and S2. We assessed the connectivity from each ROI to other voxels over the whole brain using the psycho-physiological interaction analysis (PPI) (Friston et al., 1997; O'Reilly et al., 2012). In particular, we used a generalized PPI analysis (gPPI) to improve sensitivity and specificity (McLaren et al., 2012). In the gPPI analysis, we extracted the first eigenvariate BOLD signal from each ROI and deconvolved it using the canonical HRF to obtain an approximation of neural activity. Next, we centered the resulting time series of neural activity and multiplied it by the psychological factors defined as {Test vs Baseline} and {Control vs Baseline}. This psychologically factored neural activity was termed the interaction time series. Finally, we convolved the interaction time series with the canonical HRF again, generating a hemodynamic-level interaction variable (called a PPI term). We reconstructed an individual-level design matrix by incorporating regressors for the PPI terms and the extracted time series of the local ROI, along with the initial set of regressors used for the contrast analysis, including task onset, onset of subjects' response and head motion parameters. Then, we applied a GLM to predict the BOLD signals of a target voxel from this design matrix. We computed the contrast of the PPI regressors for {Test vs Baseline} and {Control vs Baseline} using the paired t-test in each subject and utilized the obtained contrast images for subsequent group analysis. Through this analysis, we identified connectivity differences between the test and control stimuli that differed in the presence or absence of assimilation. To evaluate statistical significance, we set the height threshold at $p = 0.001$ (uncorrected) and corrected the extent threshold of activation to $p < 0.05$, accounting for multiple comparisons across the whole brain using FWE correction. This analysis allowed us to identify regions that exhibited significant connectivity changes between the test and control conditions for each of the AF and AH conditions.

After identifying brain regions showing significant inter-regional connectivity with somatosensory cortical ROIs by the gPPI analysis, we assessed relationships with individual level behavioral assimilation effects. This allows us to test the null hypothesis that connectivity in regions showing significant differences is not correlated with individual PSEs. Similar to the PSC analysis above, we used individual differences in the PSE between the test and control conditions. We defined individual connectivity by averaging the difference of the beta estimates of the gPPI between the two conditions in the identified brain regions. We calculated the Pearson correlation coefficient between individual connectivity and the PSE difference across subjects. Brain connectivity results were rendered on a three-dimensional brain surface using the BrainNetViewer toolbox (www.nitrc.org/projects/bnv/) (Xia et al., 2013).

3. Results

3.1. Induction of the assimilation effect

In accord with a previous study (Kuroki et al., 2017), behavioral outcomes reflecting the assimilation effect were observed in both the AF and AH conditions as evidenced by a shift in the psychometric function towards higher frequencies under the test conditions (Aft and AHt) where the distractor frequency was greater than the target frequency (200 Hz vs 30 Hz) compared to the ND condition and the control conditions (AFc and AHc) where distractor frequency was equal to the target frequency (Fig. 4A, B and Fig. S1). One-way rmANOVA revealed a significant effect on PSE under ND and AF conditions (AFc and AFt) ($F(2, 56) = 11.142$, $p=0.00008$). Tukey's post-hoc test showed that the PSE was significantly higher in the AFt condition (mean ± SEM, 33.95 ± 5.35 Hz,) than the ND condition (29.27 ± 3.51 Hz, $p = 0.002$) and the AFc condition (28.63 ± 4.42 Hz, $p = 0.0006$), indicating that the perceived target frequency was greater than the actual target frequency under test condition (Fig. 4C). Likewise, a one-way rmANOVA revealed a significant effect of the ND and AH conditions (AHc and AHt) on the PSE ($F(2,56) = 8.959$, $p = 0.0004$). Tukey's post-hoc test showed that the PSE was higher in the AHt condition (32.68 ± 4.15 Hz) than the ND condition (29.27 ± 3.51 Hz, $p = 0.002$) and the AHc condition (29.40 ± 3.93 Hz, $p = 0.005$) (Fig. 4D). These results indicated that the assimilation effect also occurred across hands. Although the PSE in the AHt condition was slightly smaller than that in the AFt condition, the difference was not significant (paired t-test, $t(28) = 0.924$, $p = 0.363$).

3.2. Regional neural activations associated with the vibrotactile stimulation

As expected, contrast analysis of stimuli versus baseline showed that vibrotactile stimuli activated the somatosensory cortical regions. All

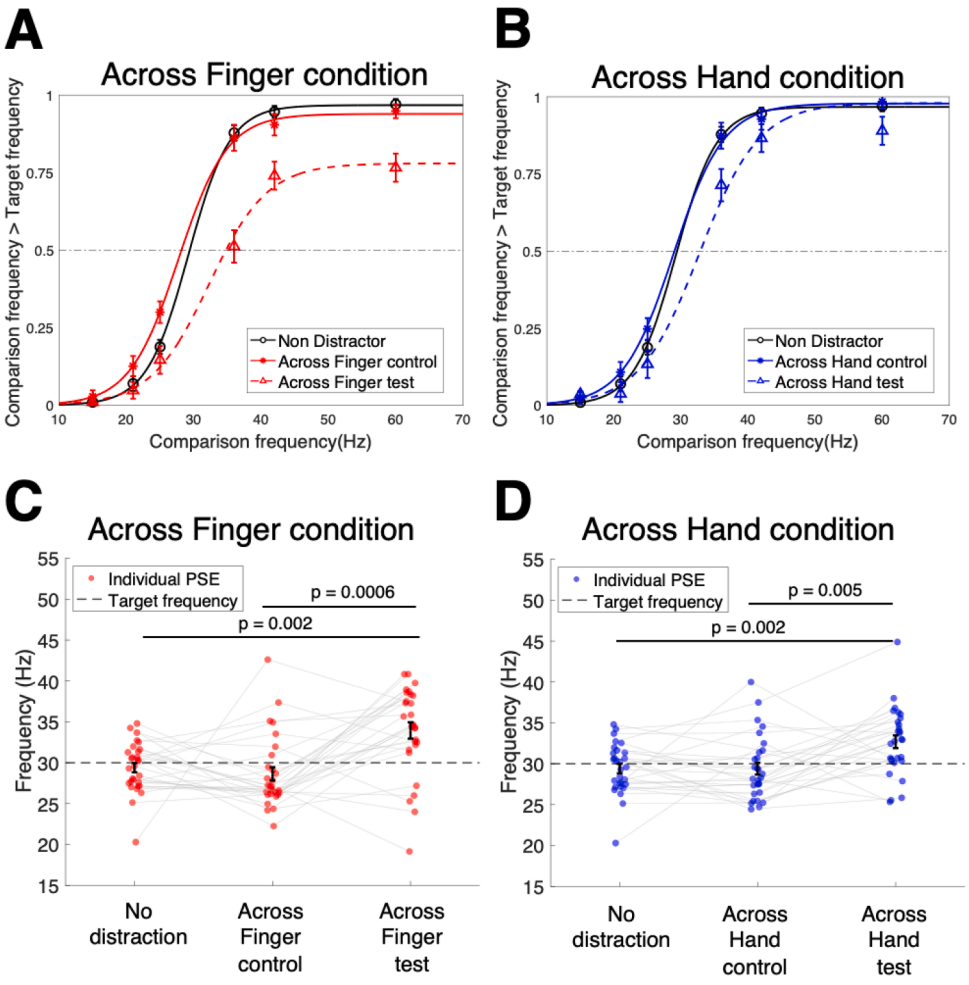

Fig. 4. Behavioral results of assimilation effects. (A) Psychometric functions for the across-finger control and test conditions (AFc and AFt conditions). The mean proportion of trials in which subjects judged that the comparison stimulus vibrated at a higher frequency than the target stimulus (30 Hz) is marked on the vertical axis for six different comparison stimuli: 15, 21, 25, 35, 42, and 60 Hz ($N = 29$ subjects). The psychometric functions of the non-distractor condition (ND, black open circle) and the control (AFc, red star) conditions are similar, while the psychometric function of the test (AFt, red triangle) condition is deviant. (B) Psychometric functions for across-hand control and test conditions (AHc and AHt conditions). Again, the psychometric functions of the ND (black open circle) and the control (AHc, red star) conditions are similar, while the psychometric function of the test (AHt, red triangle) condition is deviant. (C) The mean point of subject equality (PSE) values in the AF conditions. (D) Mean PSE values in the AH conditions. Error bars indicate the standard error.

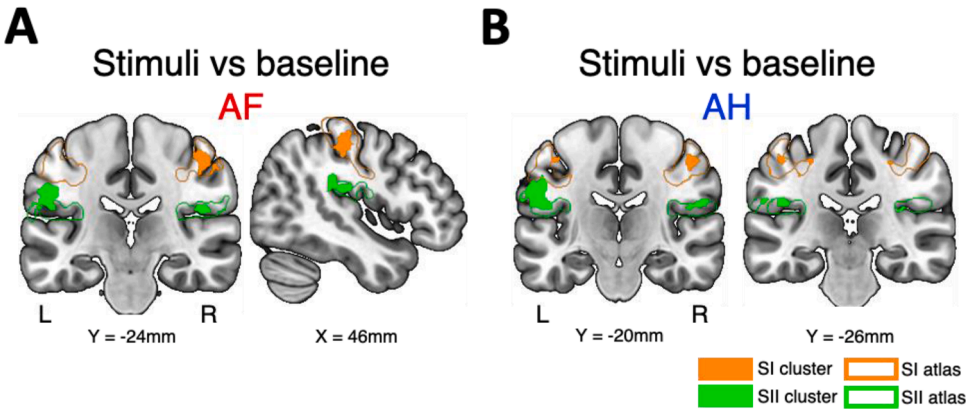

Fig. 5. Brain regions activated by vibrotactile stimuli compared to baseline. The S1 (orange outline) and S2 (green outline) were defined according to the Juelich atlas (Amunts et al., 2020). The filled-in areas indicate parts of S1 (orange) and S2 (green) that showed significant activation in response to the stimulus compared to the baseline. (A) Response maps showing somatosensory cortices activated by all the vibrotactile stimuli in the across-finger (AF) condition compared to baseline. Right S1 contralateral to the stimuli and bilateral S2 regions showed significant responses. (B) Response maps of the stimuli vs baseline contrast in the across-hands (AH) condition. The bilateral S1 and bilateral S2 regions show significant responses. The significance of activation was corrected for multiple comparisons ($p < 0.05$) at the cluster level with a height threshold ($p < 0.001$) at the voxel level.

contrast results followed the same threshold criteria (FWE corrected $p < 0.05$, cluster size > 10, cluster defining threshold $p < 0.001$). In the AF condition, the bilateral S2 and contralateral S1 showed significant activation by the vibrotactile stimulation during the target period (Fig. 5A). Additional significant responses were observed in other regions including the precentral gyrus, occipital lobe, N motor area, cerebellum, insula, and inferior frontal lobe (Table 1). In the AH condition, bilateral S1 and bilateral S2 showed significant activation by the vibrotactile stimulation during the target period (Fig. 5B). In addition, occipital lobe and left precentral gyrus were also activated (Table 1). Bilateral S2 was also significantly activated during both AHt and AFt conditions compared to corresponding control conditions (Table 1).

3.3. Percent signal changes in the somatosensory cortex

We defined individual local ROIs in the activated regions identified by the stimulus versus baseline contrast analysis. Then, we measured the PSC of each ROI and calculated the difference in PSC between the test and control conditions. Two-way rmANOVA revealed no significant main effect of the AF conditions (region: $F(2,56) = 0.179$, $p = 0.837$; condition: $F(1,28) = 4.089$, $p = 0.053$) and no significant condition x region interaction effect ($F(2,56) = 0.502$, $p = 0.608$) (Fig. 6A). There was also no significant main effect of AH conditions (region: $F(3,84) = 0.506$, $p = 0.679$; condition: $F(1,28) = 2.649$, $p = 0.115$), but there was a significant condition × region interaction effect ($F(3, 84) = 5.389$, $p = 0.002$). Tukey's post-hoc test showed a significant difference in the left S2 ($p = 0.007$) between the AHt and AHc conditions (Fig. 6B). However, correlation analysis revealed that the PSC difference between the test and control conditions was not significantly correlated with the PSE difference across subjects in any ROI (Fig. 6C). Although significant activation was found in the left S2 under the AH condition, the no significant correlation with behavioral measures suggests that local activity alone may not account for the assimilation effect. Therefore, we next examined whether inter-regional connectivity could better explain this assimilation effect.

Table 1
Summary of the group-level contrast analysis. The 3D MNI coordinates and t-values of each cluster peak point are listed. The significance of activation was corrected for multiple comparisons ($p < 0.05$ at the cluster level), with a height threshold ($p < 0.001$) at the voxel level. M1: Precentral cortex, S1: Primary somatosensory cortex, S2: Secondary somatosensory cortex.

Brain region	Coordinates			T value
	x	y	z	
Across Finger (Stimuli vs Baseline)				
Right S1	50	-20	50	7.38
	46	-26	46	5.09
	42	-22	54	4.57
Left S2	-50	-22	30	5.72
	-54	-16	18	5.09
	-56	6	32	4.41
Right S2	46	-22	20	4.90
	42	-32	28	4.76
Left M1	-52	6	24	5.72
	-58	4	16	5.55
	-56	6	32	5.51
Left lnsular	-30	18	10	5.11
Across Hand (Stimuli vs Baseline)				
Left S1	-46	-26	50	4.72
Right S1	48	-18	50	7.07
Left S2	-48	-20	20	6.85
Right S2	58	-18	22	4.81
Left Occipital cortex	-16	-86	-8	6.34
Right Occipital cortex	36	-84	-8	5.78
Left Premotor	-56	10	18	4.93
Right Premotor	58	8	20	5.65
Across Finger (Test vs control)				
Left S2	46	-14	22	5.16
Right S2	52	-24	26	4.47
Across Hand (Test vs control)				
Left S2	66	-22	22	5.94
Right S2	-58	-24	20	5.2

3.4. Connectivity between the somatosensory cortex and other regions

Using the gPPI analysis, we searched for brain regions exhibiting increased functional connectivity with the local ROIs within the somatosensory cortex under the test condition compared to the control condition. All gPPI results followed the same threshold criteria (FWE corrected $p < 0.05$, cluster size > 10, cluster defining threshold $p < 0.001$). In the AF condition, the local ROI in the right S1 showed significant connectivity with the medial prefrontal cortex (mPFC) and the left inferior parietal lobule (IPL) (Fig. 7A). However, no significant connectivity was observed with other local ROIs in the bilateral S2. In the AH condition, the local ROI in left S2 showed significant connectivity with the mPFC, right IPL, precuneus, and left temporal sulcus (Fig. 7B). The local ROIs in left S1, right S1, and right S2 did not show significant changes in connectivity with any other brain regions. These findings suggest that distractor stimuli alter brain connectivity with specific somatosensory regions. Alternatively, we found no brain regions exhibiting significantly reduced connectivity with the local ROIs in the somatosensory cortex under the test condition compared to the control condition.

We examined the correlations between individual connectivity and individual PSE differences for each inter-regional connection identified by the gPPI analysis above. In the AF condition, individual connectivity between the right S1 and mPFC showed a significant negative correlation with the PSE difference ($df = 27$, $p = 0.014$, $r = -0.45$, uncorrected) (Fig. 8A). In the AH condition, connectivity between the left S2 and right IPL showed a significant positive correlation with the PSE difference ($df = 27$, $p = 0.036$, $r = 0.39$, uncorrected) (Fig. 8B). Other inter-regional connections did not show significant correlations with the PSE difference ($p > 0.05$). These results suggest that the assimilation effect can be attributed to changes in connectivity between the somatosensory region and other higher-order brain areas.

4. Discussion

Behavioral studies have demonstrated that distractor tactile stimuli can bias perception of a target tactile stimulus, termed a tactile assimilation effect (Kahrimanovic et al., 2009; Kuroki et al., 2017), but the underlying neural mechanisms had not been studied extensively. The present study aimed to identify both localized brain activations and inter-regional functional connectivity associated with the assimilation effect. We successfully replicated the vibrotactile assimilation effect reported by Kuroki et al. (2017) as evidenced by significantly higher PSE values under the AF and AH test conditions compared to the ND and corresponding AF and AH control conditions. Also, we observed a significant increase in PSC in the left S2 under the AHt condition, supporting our hypothesis that the stimuli inducing assimilation would elicit a greater BOLD response. However, PSC did not significantly correlate with PSE differences, suggesting that local activation may not directly reflect perceptual assimilation. We further found that inter-regional connectivity between the somatosensory cortex and other brain regions was increased by the presence of the distractor stimulus. Notably, stronger assimilation was associated with weaker right S1–mPFC connectivity in the AF condition and stronger left S2–IPL connectivity in the AH condition. Therefore, these results suggest that the vibrotactile assimilation effect is associated with interactions between the somatosensory cortex and higher-order brain regions.

4.1. Neural activation patterns in the somatosensory cortex induced by the distractor stimulus

The regions of primary and secondary somatosensory cortex

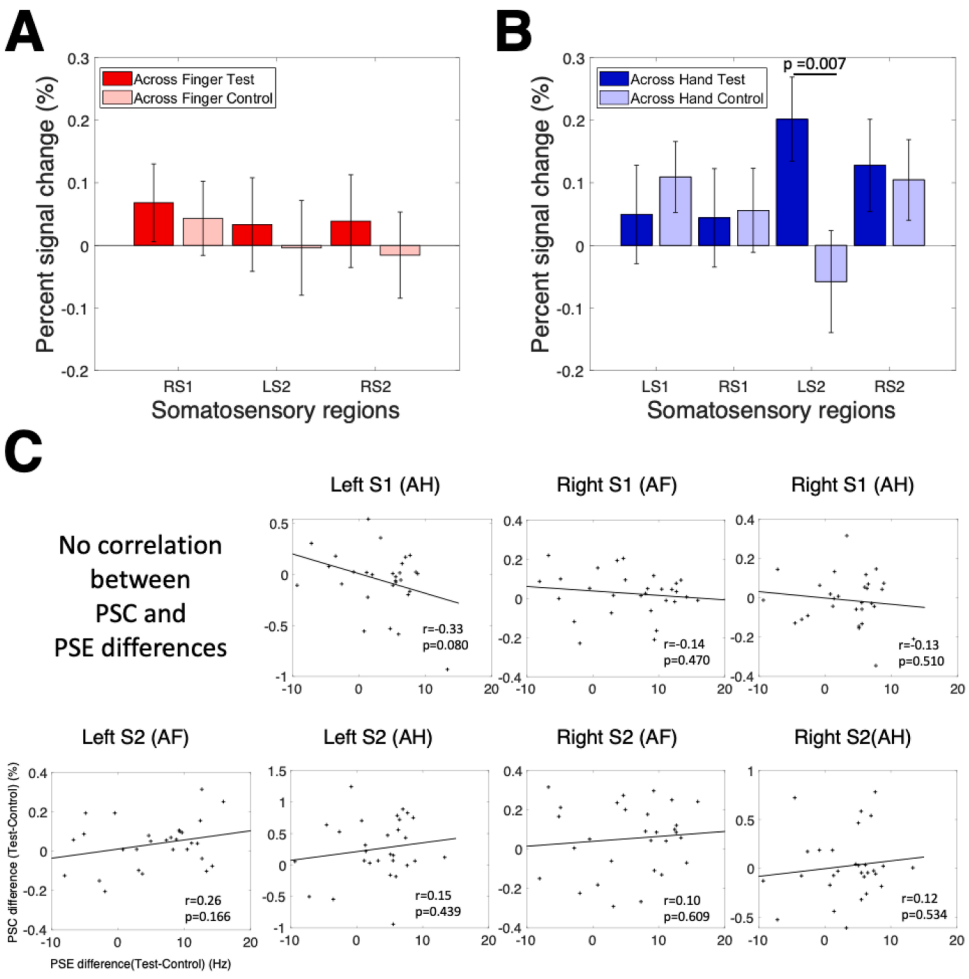

Fig. 6. The percent signal changes (PSCs) in the somatosensory regions and correlations with point of subject equality (PSE) values. (A) The mean PSCs in the right S1 (RS1), left S2 (LS2), and right S2 (RS2) regions under the across-finger test and control (AFt and AFc) conditions. PSC differences were not significant between the test and control conditions in any somatosensory regions. Error bars denote the standard error of the mean. (B) Mean PSCs in left S1 (LS1), RS1, LS2, and RS2 regions under the across-hands test and control (AHt and AHc) conditions. The PSC in LS2 differed significantly between the test and control conditions, while no differences were found in other somatosensory regions. (C) Correlations of PSE differences between test and control with PSC differences between test and control conditions in three regions of interest under the AF condition and four regions of interest under the AH condition. No region showed a significant correlation (df=27, ps>0.05). Each dot denotes the data point of an individual subject ($N = 29$).

responding to vibrotactile finger stimulation of the left or both hands were consistent with previous studies (Chung et al., 2013; Lamp et al., 2018; Lee et al., 2016). Among these somatosensory cortices, left S2 under the AH condition was increased when the distractor stimulus was presented together with the target stimulus. As S2 is reportedly involved in the integration of somatosensory information (Zhu et al., 2007), the observed elevation in BOLD signal reflect the integration of tactile information from the RA-I and RA-II afferents from distinct fingers. However, it is also possible that elevated S2 activation simply reflects the higher frequency of the distractor stimulus (200 Hz in this study), as many studies reported more prominent neural responses in S2 to high-frequency vibration than to low-frequency flutter (Chung et al., 2013; Francis et al., 2000; Harrington and Hunter Downs, 2001). In addition, these results may reflect activation of larger receptive field by higher frequency stimuli. Suprathreshold high-frequency stimulation is more likely to activate RA-II mechanoreceptors with larger receptive fields (Sherrick et al., 1990). Furthermore, S2 responds bilaterally even to unilateral stimulation, indicating the presence of broad receptive fields. (Ruben et al., 2001). These properties may account for the greater activation observed in the left S2, where we observed a significant difference in PSC between the test and control conditions under the AH stimulation conditions. Thus, the 200-Hz tactile stimulus delivered as a distractor in the test condition may have induced larger S2 responses compared to the control condition (where only 30-Hz stimulation was delivered) independent of the assimilation effect.

To address this potential compound, we may need to test whether the contrast of the test against control still activates S2 in the opposite condition when a high-frequency target stimulus (e.g., 200 Hz) and a low-frequency distractor stimulus (e.g., 30 Hz) are presented. However, we could not employ this regimen due to the resonance over 200 Hz generated by the PTS (see section 2.2. *Vibrotactile stimuli*). In addition, we observed that individual PSC differences in S2 were not significantly correlated with individual PSE values (Fig. 6). The absence of a significant correlation between individual assimilation effect (PSE values) and neural responses in right S2 under the AF condition or in the left S2 under the AH condition also suggests that neural processing of vibrotactile signals in S1 and S2 does not directly reflect the assimilation effect.

4.2. *Brain connectivity changes associated with the across-finger assimilation effect*

We found significant differences in connectivity between the right S1 and left IPL and between right S1 and mPFC between the AF test and

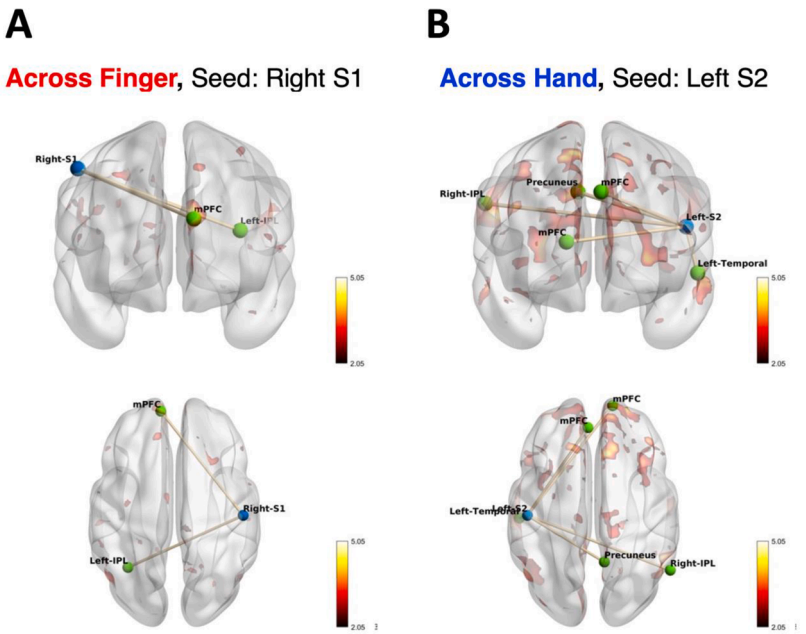

Fig. 7. Brain connectivity results by the gPPI analysis. (A) Under the AF condition, the gPPI analysis revealed two significant connections from the right S1 (seed region) to the mPFC and left IPL. No significant connectivity was found when the left S2 or right S2 was used as a seed region. (B) Under the AH condition, gPPI analysis revealed four significant connections from left S2 to mPFC, right IPL, precuneus, and left temporal sulcus. No significant connectivity was found for left S1, right S1, and right S2 as a seed region. Significant connectivity was indicated by $p < 0.05$ corrected for multiple comparisons at the cluster level, with a height threshold at the voxel level of $p < 0.001$. The blue node indicates the seed ROI, and the green nodes indicate the brain regions showing significant connectivity with the seed ROI. The color scale indicates the t-values of the gPPI results.

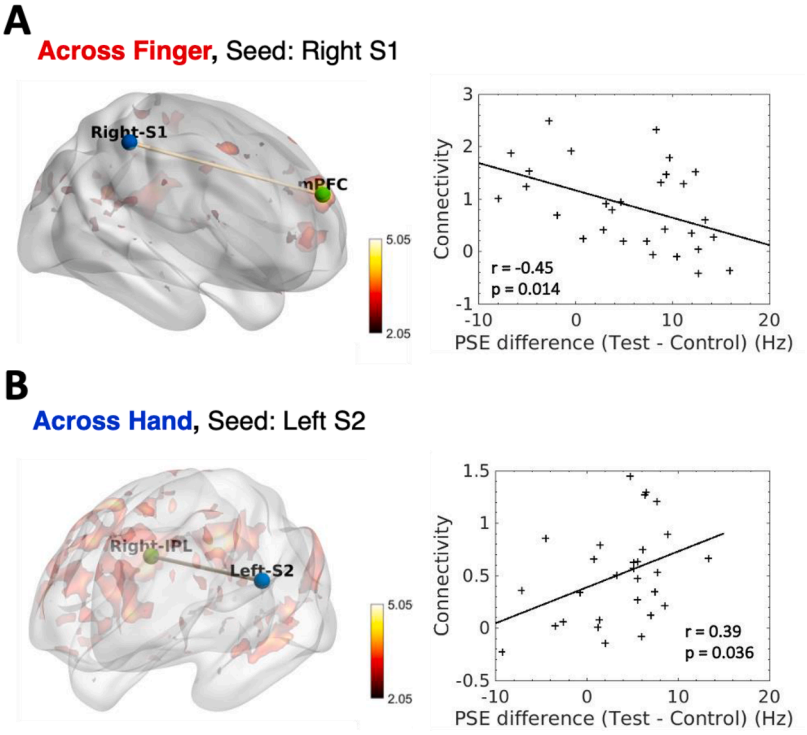

Fig. 8. Correlations between individual PSE and brain connectivity. (A) Individual connectivity between right S1 and mPFC shows a significant negative correlation with individual PSEs under the AF condition. (B) Individual connectivity between left S2 and right IPL shows a significant positive correlation with individual PSEs under the AH condition. The blue node indicates the seed ROI, and the green nodes indicate the brain regions that show significant connectivity with the seed ROI. The color scale indicates the t-value of the gPPI analysis. Each dot denotes results from an individual subject ($N = 29$).

control conditions. The involvement of structural and functional connectivity between S1 and IPL for tactile perception is well documented (Andersen et al., 1990; Rolls et al., 2023). While the regional activities of IPL and S1 did not increase significantly, connectivity increased in response to RA-I and RA-II inputs, indicating that S1 and IPL activity became more strongly associated when both the target and distractor

stimuli were presented than when only the target stimulus was presented. However, no significant correlation between individual connectivity and PSE was found across subjects, suggesting that increased connectivity between S1 and IPL represents the transmission of multiple types of tactile signals.

We also found significant increases in connectivity between the right S1 and mPFC. In contrast to S1-IPL connectivity, individual connectivity between S1 and mPFC showed a significant negative correlation with individual PSE. It suggests the engagement of S1-mPFC connectivity in the occurrence of the assimilation effect. Previous research has shown that S1-mPFC connectivity is positively correlated with congruency between multisensory stimuli during recognition memory tasks (Van Kesteren et al., 2010). Based on this report, we speculate that subject experiencing distraction by the 200-Hz stimulus during the perception of the 30-Hz stimulus in the test condition, the perception of the 30-Hz stimulus to which subjects paid attention might be more dissimilar between the test and control conditions, increasing incongruency between the perception of the 30-Hz stimulus with and without distractor (note that test and control trials were randomly mixed in a block). As such, S1-mPFC connectivity in these highly distracted subjects would be weaker and the assimilation effect stronger.

4.3. Brain connectivity changes associated with the across-hands assimilation effect

In the AH condition, target and distractor stimuli altered the connectivity between left S2 and mPFC, precuneus, left temporal sulcus, and right IPL, all brain regions implicated in tactile perception. The precuneus is involved in the detection of incongruent tactile stimuli (Kitada et al., 2014). The temporal sulcus reportedly responds to vibrotactile stimulation (Beauchamp et al., 2008; Hegner et al., 2007) and contributes to the integration of multisensory information (Renier et al., 2009). IPL contributes to the recognition of tactile stimuli and object shapes (Jäncke et al., 2001). Further, functional connectivity between the IPL and S2 has been reported during a tactile memory task (Kostopoulos et al., 2007).

However, only the left S2 and right IPL connectivity showed a significant positive correlation with individual PSE. Previous studies reported increased connectivity between S2 and IPL during tactile object recognition (Yu et al., 2018) and vibrotactile stimulation (Chung et al., 2013). IPL is involved in integrating sensory information (Clower et al., 2001). Based on these findings, we speculate that individuals exhibiting greater perceptual bias (with a stronger assimilation effect) are less likely to suppress perception of the distractor stimulus on the unattended hand and require increased connectivity between the left S2 and right IPL to attend to both vibrotactile inputs. That the assimilation effect modulated the connectivity between S2 and IPL across hemispheres further suggests that transhemispheric connectivity may be engaged in the emergence of the across-hand assimilation effect. Building on the findings from the across-finger condition, we conclude that the assimilation effect can be explained by changes in connectivity between the somatosensory cortices and both parietal and frontal brain regions.

4.4. Differences in neural substrates between the across-finger and across-hand assimilation effects

We found a negative correlation between right S1–mPFC connectivity and individual PSE in the AF condition, and a positive correlation between left S2–right IPL connectivity and PSE in the AH condition. However, we confirmed that individual PSE changes from the control to test conditions were not significant correlation between the AF and AH conditions (df = 27, p=0.316, r=-0.19) (Fig. 9). This result implying that individuals who exhibited a stronger assimilation effect under the AF condition did not necessarily show a stronger assimilation effect under the AH condition. Furthermore, other studies have reported different activation patterns in S1 and S2 when a pair of vibrotactile

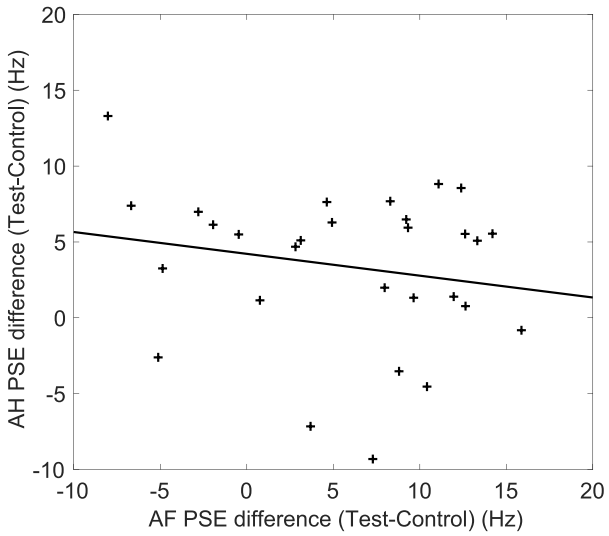

Fig. 9. Correlation between AF and AH PSE differences. The individual PSE differences between the test and control AF conditions do not show a correlation with those between the test and control AH conditions (df=27, p=0.316, r=-0.19). Each dot denotes a value from an individual subject (N=29).

stimuli were presented to one hand or both hands (Tamè et al., 2014). Taken together, our results imply that the AF and AH assimilation effects involve different neural circuits.

4.5. Why assimilation, not contrast effects with vibrotactile stimulation?

The assimilation effect describes a perceptual bias toward the distractor stimulus, while the contrast effect refers to a perceptual bias away from the distractor (Kahrimanovic et al., 2009). Among these, the assimilation effect occurred when vibrotactile stimuli with different frequencies were presented. Kahrimanovic et al. (2009) also reported the assimilation effect by tactile stimulations such that when both the control stimulus and a soft or rough stimulus were presented to the adjacent fingers simultaneously, subjects showed the assimilation effect of responding to the control stimulus as softer or rougher. Linking to the visual assimilation effect, Kahrimanovic et al. (2009) posited that receptive field overlap in the somatosensory cortex may contribute to the assimilation of tactile perceptions. If tactile stimuli are presented to the index and middle fingers, regions with closely spaced receptive fields, the brain may sum the stimuli and perceptually assimilate the averaged signal.

Likewise, under the AF condition, we speculate that the vibrotactile afferent signals in the receptive fields of the index and middle fingers may be averaged in S1. Then, S1 transmits this averaged signal (greater than that in response to the target stimulus alone) to the mPFC for tactile discrimination, which leads to the perception of incongruent tactile stimuli and decreased connectivity. However, this assumption about the proximity of the receptive fields may not apply to the assimilation effect under the AH condition because it is unknown whether the receptive fields of two different index fingers are close to each other within S2. Thus, the vibrotactile assimilation effect may need to be elucidated by more complex neural processing than a simple mixture of receptive fields.

4.6. Using the canonical HRF in the GLM analysis of short-lasting stimuli

We employed the canonical HRF in our analysis because previous fMRI studies investigating neural responses to sensory stimuli lasting less than 1 second also used only the canonical HRF (Kimura et al., 2019; Wang et al., 2023; Wittkuhn and Schuck, 2021). However, we recognize that incorporating the derivatives of the HRF into the GLM could

potentially alter the neural activation results, as demonstrated in prior research (Henson et al., 2002). While we acknowledge that the temporal and dispersion derivatives of the HRF may account for variations in the HRF for the short-lasting stimuli used in this study, we opted to include only the canonical HRF in the GLM. This decision was based on our observation that the GLM analysis with the canonical HRF reliably identified neural activation in the somatosensory cortex when contrasting vibrotactile stimulation versus baseline.

4.7. Limitations

The correlation coefficients between individual PSE values and connectivity were -0.45 under the AF condition and 0.39 under the AH condition. These coefficients suggest moderate correlations between behavioral and neural responses, although not notably strong. The results from the correlation analysis between individual PSE values and connectivity did not account for multiple comparisons, which may lead to less robust statistical evaluation. Possible explanations for these modest correlations might include the limited sample size and undefined factors contributing to individual variations in PSE, such as a lack of a sufficient number of trials and the effects of the MRI environment. Indeed, a sample size of 29 subjects is relatively small for demonstrating statistically significant correlation between behavioral and neural responses. For instance, if we had a larger sample size, we might be able to identify the correlation between PSE and cortical PSC rates. Nonetheless, several recent studies on tactile fMRI experiments also recruited around 20 subjects and successfully showed neural responses associated with human tactile sensation (Brodoehl et al., 2020; Kim et al., 2019). Therefore, we believe that this sample size is sufficient to accept the results.

Despite instructions to subjects to refrain from finger movements as well as visual monitoring of subjects' movements throughout the experiment, there remains a possibility that subtle movements or electromyographic (EMG) activity occurred. Research has indicated that movements can alter various aspects of tactile perception such as perceptual intensity (Voss et al., 2006) or stimulus onset timing (Jackson et al., 2011). Moreover, Williams and Chapman confirmed that EMG activation can be observed even in the absence of visible movement (Williams and Chapman, 2002). Another study found that attenuated neural responses can be detected even when there is no movement (Arikan et al., 2021). Despite potential impacts of movement on tactile perception, it is likely that any movements or EMG activity occurred randomly across experimental conditions, presumably canceling out their effects in the contrast analysis between conditions. Hence, we speculate that the vibrotactile assimilation effect on tactile perception was minimally influenced by movement or EMG activity in this study. Nevertheless, further investigation is warranted to explore any potential relationship between the vibrotactile assimilation effect and movement.

We instructed subjects to press the left pad if the target stimulus felt higher, and the press right pad if the comparison stimulus felt higher. These response modes may have unintentionally introduced a lateralized effect. To minimize this potential confounding factor, we included the onset of each subject's foot pad press as a nuisance regressor in the first-level GLM, thereby accounting for the response-related neural activity. As a result, no lateralized BOLD responses were found in any contrast (stimulus vs. baseline, test vs. control, or trials with >30 Hz vs. <30 Hz comparison stimuli), suggesting that the behavioral response mode did not bias our neuroimaging results.

Declaration of generative AI and AI-assisted technologies in the writing process

During the preparation of this work the author(s) used ChatGPT in order to proofread the manuscript. After using this tool/service, the author(s) reviewed and edited the content as needed and take(s) full responsibility for the content of the publication.

CRediT authorship contribution statement

Ji-Hyun Kim: Writing – original draft, Visualization, Validation, Software, Methodology, Investigation, Formal analysis, Data curation, Conceptualization. **Dooyoung Jung:** Investigation, Funding acquisition, Formal analysis, Data curation. **Junsuk Kim:** Writing – review & editing, Validation, Software, Methodology, Investigation, Formal analysis, Conceptualization. **Sung-Phil Kim:** Writing – review & editing, Supervision, Project administration, Funding acquisition, Conceptualization.

Declaration of competing interest

The authors declare that there are no competing financial interests regarding the publication of this paper.

Acknowledgments

This research was supported by the Brain Research Program through the National Research Foundation of Korea (NRF) funded by the Ministry of Science, ICT & Future Planning (2022M3C7A1015112), the National Research Foundation of Korea (NRF) grants funded by the Korea government (MSIT) (No. RS-2023-00302489), the Alchemist Project (20012355, Fully implantable closed loop Brain to X for voice communication) funded by the Ministry of Trade, Industry & Energy (MOTIE, Korea), and IITP(Institute of Information & Coummunications Technology Planning & Evaluation)-ITRC(Information Technology Research Center) grant funded by the Korea government(Ministry of Science and ICT)(IITP-2025-00437866). The authors would like to thank Enago(w ww.enago.com) for the English language editing.

Supplementary materials

Supplementary material associated with this article can be found, in the online version, at doi:10.1016/j.neuroimage.2025.121310.

Data availability

Subject data has been anonymized and publicly available on 'OpenNeuro' (10.18112/openneuro.ds005941.v1.0.0). The behavioral data and analysis code are released at (https://github.com/ji-hyun-fmri/Assimilation).

References

Abraira, V.E., Ginty, D.D., 2013. The sensory neurons of touch. Neuron 79, 618–639. https://doi.org/10.1016/j.neuron.2013.07.051.

Acaster, S.L., Taroyan, N.A., Soranzo, A., Reidy, J.G., 2021. Behavioral and electrophysiological correlates of lightness contrast and assimilation. Exp. Brain Res. 3205–3220. https://doi.org/10.1007/s00221-021-06197-3.

Amunts, K., Mohlberg, H., Bludau, S., Zilles, K., 2020. Julich-Brain: a 3D probabilistic atlas of the human brain's cytoarchitecture. Science 369 (6506), 988–992. https://doi.org/10.1126/science.abb4588.

Andersen, R.A., Asanuma, C., Essick, G., Siegel, R.M., 1990. Corticocortical connections of anatomically and physiologically defined subdivisions within the inferior parietal lobule. J. Comp. Neurol. 29665, 13. https://doi.org/10.1002/cne.902960106, 1.

Arikan, B.E., Voudouris, D., Voudouri-Gertz, H., Sommer, J., Fiehler, K., 2021. Reach-relevant somatosensory signals modulate activity in the tactile suppression network. Neuroimage 236, 118000. https://doi.org/10.1016/j.neuroimage.2021.118000.

Beauchamp, M.S., Yasar, N.E., Frye, R.E., Ro, T., 2008. Touch, sound and vision in human superior temporal sulcus. Neuroimage 41 (3), 1011–1020. https://doi.org/10.1016/j.neuroimage.2008.03.015.

Bensmaïa, S., Hollins, M., 2005. Pacinian representations of fine surface texture. Percept. Psychophys. 67, 842–854. https://doi.org/10.3758/BF03193537.

Blankenburg, F., Ruff, C.C., Deichmann, R., Rees, G., Driver, J., 2006. The cutaneous rabbit illusion affects human primary sensory cortex somatotopically. PLoS Biol. 4, e69. https://doi.org/10.1371/journal.pbio.0040069.

Brett, M., Anton, J.-L., Valabreque, R., Poline, J.-B., 2002. Region of interest analysis using an SPM toolbox. In: Paper presented at the Eighth International Conference on Functional Mapping of the Human Brain. Sendai, Japan. June.

Brodoehl, S., Gaser, C., Dahnke, R., Witte, O.W., Klingner, C.M., 2020. Surface-based analysis increases the specificity of cortical activation patterns and connectivity results. Sci. Rep. 10. https://doi.org/10.1038/s41598-020-62832-z.
Chen, L.M., Friedman, R.M., Ramsden, B.M., LaMotte, R.H., Roe, A.W., 2001. Fine-scale organization of SI (area 3b) in the squirrel monkey revealed with intrinsic optical imaging. J. Neurophysiol. 86, 3011–3029. https://doi.org/10.1152/JN.2001.86.6.3011/ASSET/IMAGES/LARGE/9K1212025009.JPEG.
Chen, L.M., Friedman, R.M., Roe, AW., 2003. Optical imaging of a tactile illusion in area 3b of the primary somatosensory cortex. Science 302 (5646), 881–885. https://doi.org/10.1126/scienc.1087846.
Chung, Y.G., Kim, J., Han, S.W., Kim, H.S., Choi, M.H., Chung, S.C., Park, J.Y., Kim, S.P., 2013. Frequency-dependent patterns of somatosensory cortical responses to vibrotactile stimulation in humans: A fMRI study. Brain Res. 1504, 47–57. https://doi.org/10.1016/J.BRAINRES.2013.02.003.
Clower, D.M., West, R.A., Lynch, J.C., Strick, P.L., 2001. The inferior parietal lobule is the target of output from the superior colliculus, hippocampus, and cerebellum. J. Neurosci. 21, 6283–6291. https://doi.org/10.1523/jneurosci.21-16-06283.2001.
Davidenko, O., Bonny, J.M., Morrot, G., Jean, B., Claise, B., Benmoussa, A., Fromentin, G., Tomé, D., Nadkarni, N., Darcel, N., 2018. Differences in BOLD responses in brain reward network reflect the tendency to assimilate a surprising flavor stimulus to an expected stimulus. Neuroimage 183, 37–46. https://doi.org/10.1016/j.neuroimage.2018.07.058.
Dykes, R.W., Sur, M., Merzenich, M.M., Kaas, J.H., Nelson, R.J., 1981. Regional segregation of neurons responding to quickly adapting, slowly adapting, deep and pacinian receptors within thalamic ventroposterior lateral and ventroposterior inferior nuclei in the squirrel monkey (Saimiri sciureus). Neuroscience 6, 1687–1692. https://doi.org/10.1016/0306-4522(81)90235-9.
Eickhoff, S.B., Grefkes, C., Zilles, K., Fink, G.R., 2007. The somatotopic organization of cytoarchitectonic areas on the human parietal operculum. Cereb. Cortex 17, 1800–1811. https://doi.org/10.1093/cercor/bhl090.
Francis, S.T., Kelly, E.F., Bowtell, R., Dunseath, W.J.R., Folger, S.E., McGlone, F., 2000. fMRI of the responses to vibratory stimulation of digit tips. Neuroimage 11, 188–202. https://doi.org/10.1006/NIMG.2000.0541.
Friedman, R.M., Chen, L.M., Roe, A.W., 2004. Modality maps within primate somatosensory cortex. Proc. Natl. Acad. Sci. USA. 101, 12724–12729. https://doi.org/10.1073/PNAS.0404884101.
Friston, K.J., Buechel, C., Fink, G.R., Morris, J., Rolls, E., Dolan, R.J., 1997. Psychophysiological and Modulatory Interactions in Neuroimaging. Neuroimage 6, 218–229. https://doi.org/10.1006/nimg.1997.0291.
Harrington, G.S., Hunter Downs, J., 2001. FMRI mapping of the somatosensory cortex with vibratory stimuli: is there a dependency on stimulus frequency? Brain Res. 897, 188–192. https://doi.org/10.1016/S0006-8993(01)02139-4.
Hartmann, S., Missimer, J.H., Stoeckel, C., Abela, E., Shah, J., Seitz, R.J., Weder, B.J., 2008. Functional connectivity in tactile object discrimination - A principal component analysis of an event related fMRI-study. PLoS One 3. https://doi.org/10.1371/journal.pone.0003831.
Hegner, Y.L., Saur, R., Veit, R., Butts, R., Leiberg, S., Grodd, W., Braun, C., 2007. BOLD adaptation in vibrotactile stimulation: Neuronal networks involved in frequency discrimination. J. Neurophysiol. 97, 264–271. https://doi.org/10.1152/JN.00617.2006.
Henson, R.N.A., Price, C.J., Rugg, M.D., Turner, R., Friston, K.J., 2002. Detecting latency differences in event-related BOLD responses: application to words versus nonwords and initial versus repeated face presentations. Neuroimage 15, 83–97. https://doi.org/10.1006/nimg.2001.0940.
Holmes, N.P., Tamè, L., 2019. Locating primary somatosensory cortex in human brain stimulation studies: systematic review and meta-analytic evidence. J. Neurophysiol 121 (1), 152–162. https://doi.org/10.1152/jn.00614.2018.
Jackson, S.R., Parkinson, A., Pears, S.L., Nam, S.-H., 2011. Effects of motor intention on the perception of somatosensory events: a behavioural and functional magnetic resonance imaging study. Q. J. Exp. Psychol. 64, 839–854. https://doi.org/10.1080/17470218.2010.529580.
Jäncke, L., Kleinschmidt, A., Mirzazade, S., Shah, N.J., 2001. The Role of the Inferior Parietal Cortex in Linking the Tactile Perception and Manual Construction of Object Shapes. Cereb. Cortex 114–121. https://doi.org/10.1093/cercor/11.2.114.
Jeong, J., Kim, J.H., Kim, S.P., 2022. Tactile assimilation effect depends on individual autistic traits in healthy population. In: Paper presented at the International Conference on Society for Neuroscience. Sand Diego, USA. November.
Johansson, R.S., Flanagan, J.R., 2009. Coding and use of tactile signals from the fingertips in object manipulation tasks. Nat. Rev. Neurosci. 10, 345–359. https://doi.org/10.1038/nrn2621.
Johansson, R.S., Vallbo, Å.B., 1983. Tactile sensory coding in the glabrous skin of the human hand. Trends Neurosci. 6, 27–32. https://doi.org/10.1016/0166-2236(83)90011-5.
Johnson, K.O., 2001. The roles and functions of cutaneous mechanoreceptors. Curr. Opin. Neurobiol. 11, 455–461. https://doi.org/10.1016/S0959-4388(00)00234-8.
Kahrimanovic, M., Bergmann Tiest, W.M., Kappers, A.M.L., 2009. Context effects in haptic perception of roughness. Exp. Brain Res. 194, 287–297. https://doi.org/10.1007/s00221-008-1697-x.
Kim, Y., Usui, N., Miyazaki, A., Haji, T., Matsumoto, K., Taira, M., Nakamura, K., Katsuyama, N., 2019. Cortical regions encoding hardness perception modulated by visual information identified by functional magnetic resonance imaging with multivoxel pattern analysis. Front. Syst. Neurosci. 13. https://doi.org/10.3389/fnsys.2019.00052.
Kimura, T., Kadota, H., Kuroda, T., Funai, T.D., Iwata, M., Kochiyama, T., Miyazaki, M., 2019. Neural correlates of tactile simultaneity judgement: a functional magnetic resonance imaging study. Sci. Rep. 9, 19481. https://doi.org/10.1038/s41598-019-54323-7.
Kitada, R., Sasaki, A.T., Okamoto, Y., Kochiyama, T., 2014. Role of the precuneus in the detection of incongruency between tactile and visual texture information : A functional MRI study. Neuropsychologia 64, 252–262. https://doi.org/10.1016/j.neuropsychologia.2014.09.028.
Kostopoulos, P., Albanese, M.C., Petrides, M., 2007. Ventrolateral prefrontal cortex and tactile memory disambiguation in the human brain. Proc. Natl. Acad. Sci. USA. 104, 10223–10228. https://doi.org/10.1073/PNAS.0700253104.
Kuroki, S., Watanabe, J., Nishida, S., 2017. Integration of vibrotactile frequency information beyond the mechanoreceptor channel and somatotopy. Sci. Rep. 7. https://doi.org/10.1038/S41598-017-02922-7.
Lamp, G., Goodin, P., Palmer, S., Low, E., Barutchu, A., Carey, L.M., 2018. Activation of bilateral secondary somatosensory cortex with right hand touch stimulation: a meta-analysis of functional neuroimaging studies. Front. Neurol. 9, 1129. https://doi.org/10.3389/FNEUR.2018.01129.
Lee, S.D., Jung, Y., Chung, Y.A., Lee, W., 2016. Neural substrates in secondary somatosensory area for the perception of different tactile sensations. Int. J. Imaging Syst. Technol. 26, 85–91. https://doi.org/10.1002/ima.22160.
McLaren, D.G., Ries, M.L., Xu, G., Johnson, S.C., 2012. A generalized form of context-dependent psychophysiological interactions (gPPI): a comparison to standard approaches. Neuroimage 61, 1277–1286. https://doi.org/10.1016/j.neuroimage.2012.03.068.
Mountcastle, V.B., Talbot, W.H., Sakata, H., Hyvärinen, J., 1969. Cortical neuronal mechanisms in flutter-vibration studied in unanesthetized monkeys. Neuronal Periodicity Frequency Discriminat. 32, 452–484. https://doi.org/10.1152/JN.1969.32.3.452.
Nelder, J.A., Mead, R., 1965. A simplex method for function minimization. Comput. J. 7, 308–313. https://doi.org/10.1093/comjnl/7.4.308.
O'Reilly, J.X., Woolrich, M.W., Behrens, T.E.J., Smith, S.M., Johansen-Berg, H., 2012. Tools of the trade: psychophysiological interactions and functional connectivity. Soc. Cogn. Affect. Neurosci. 7, 604. https://doi.org/10.1093/scan/nss055.
Prins, N., Kingdom, F.A.A., John, R.S., 2018. Applying the model-comparison approach to test specific research hypotheses in psychophysical research using the Palamedes Toolbox 9, 1–14. https://doi.org/10.3389/fpsyg.2018.01250.
Prsa, M., Kilicel, D., Nourizonoz, A., Lee, K., Huber, D., 2021. A common computational principle for vibrotactile pitch perception in mouse and human. Nat. Commun. 12. https://doi.org/10.1038/s41467-021-25476-9.
Rajaei, N., Aoki, N., Takahashi, H.K., Miyaoka, T., Kochiyama, T., Ohka, M., Sadato, N., Kitada, R., 2018. Brain networks underlying conscious tactile perception of textures as revealed usig the velvet hand illusion. Hum. Brain Mapp. 39 (12), 4787–4801. https://doi.org/10.1002/hbm.24323.
Renier, L.A., Anurova, I., Volder, A.G. De, Vanmeter, J., 2009. Multisensory integration of sounds and vibrotactile stimuli in processing streams for " What " and " Where " 29, 10950–10960. https://doi.org/10.1523/JNEUROSCI.0910-09.2009.
Rolls, E.T., Deco, G., Huang, C.-C., Feng, J., 2023. The human posterior parietal cortex: effective connectome, and its relation to function. Cereb. Cortex 33, 3142–3170. https://doi.org/10.1093/CERCOR/BHAC266.
Rolls, E.T., Huang, C.-C., Lin, C.-P., Feng, J., Joliot, M., 2020. Automated anatomical labelling atlas 3. Neuroimage 206, 116189. https://doi.org/10.1016/j.neuroimage.2019.116189.
Rostamian, B., Koolani, M.R., Abdollahzade, P., Lankarany, M., Falotico, E., Amiri, M., Thakor, V., N, 2022. Texture recognition based on multi-sensory integration of proprioceptive and tactile signals. Sci. Rep. 12, 1–13. https://doi.org/10.1038/s41598-022-24640-5.
Ruben, J., Schwiemann, J., Deuchert, M., Meyer, R., Krause, T., Curio, G., Villringer, K., Kurth, R., Villringer, A., 2001. Somatotopic organization of human secondary somatosensory cortex. Cereb. Cortex 11 (5), 463–473. https://doi.org/10.1093/cercor/11.5.463.
Schellekens, W., Thio, M., Badde, S., Winawer, J., Ramsey, N., Petridou, N., 2021. A touch of hierarchy: population receptive fields reveal fingertip integration in Brodmann areas in human primary somatosensory cortex. Brain Struct Funct 226 (7), 2099–2112. https://doi.org/10.1007/s00429-021-02309-5.
Sherif, M., Taub, D., Hovland, C.I., 1958. Assimilation and contrast effects of anchoring stimuli on judgments. J. Exp. Psychol. 55, 150–155. https://doi.org/10.1037/h0048784.
Sherrick, C.E., Cholewiak, R.W., Collins, A.A., 1990. The localization of low-and high-frequency vibrotactile stimuli. J. Acoust. Soc. Am 88 (1), 169–179. https://doi.org/10.1121/1.399937.
Sur, M., Wall, J.T., Kaas, J.H., 1984. Modular distribution of neurons with slowly adapting and rapidly adapting responses in area 3b somatosensory cortex in monkeys. J. Neurophysiol. 51, 724–744. https://doi.org/10.1152/jn.1984.51.4.724.
Tamè, L., Pavani, F., Papadelis, C., Farnè, A., Braun, C., 2014. Early integration of bilateral touch in the primary somatosensory cortex. Front. Psychol. https://doi.org/10.1002/hbm.22719.
Van Kesteren, M.T.R., Rijpkema, M., Ruiter, D.J., Fernández, G., 2010. Retrieval of associative information congruent with prior knowledge is related to increased medial prefrontal activity and connectivity. J. Neurosci. 30, 15888–15894. https://doi.org/10.1523/JNEUROSCI.2674-10.2010.
Voss, M., Ingram, J.N., Haggard, P., Wolpert, D.M., 2006. Sensorimotor attenuation by central motor command signals in the absence of movement. Nat. Neurosci. 9, 26–27. https://doi.org/10.1038/nn1592.
Wang, B.A., Veismann, M., Banerjee, A., Pleger, B., 2023. Human orbitofrontal cortex signals decision outcomes to sensory cortex during behavioral adaptations. Nat. Commun. 14, 3552. https://doi.org/10.1038/s41467-023-38671-7.

Wetherill, G.B., Levitt, H., 1965. Sequential estimaiton of points on a psychometric function 18, 1–10. 10.1111/j.2044-8317.1965.tb00689.x.

Williams, S.R., Chapman, C.E., 2002. Time course and magnitude of movement-related gating of tactile detection in humans. III. Effect of motor tasks. J. Neurophysiol. 88, 1968–1979. https://doi.org/10.1152/jn.2002.88.4.1968.

Wittkuhn, L., Schuck, N.W., 2021. Dynamics of fMRI patterns reflect sub-second activation sequences and reveal replay in human visual cortex. Nat. Commun. 12, 1795.

Woo, C.-W., Krishnan, A., Wager, T.D., 2014. Cluster-extent based thresholding in fMRI analyses. Neuroimage 91, 412–419. https://doi.org/10.1016/j.neuroimage.2013.12.058.Cluster-extent.

Xia, M., Wang, J., He, Y., 2013. BrainNet Viewer: a network visualization tool for human brain connectomics. PLoS One 8, e68910. https://doi.org/10.1371/journal.pone.0068910.

Yarkoni, T., Poldrack, R.A., Nichols, T.E., Van Essen, D.C., Wager, T.D., 2011. Large-scale automated synthesis of human functional neuroimaging data. Nat. Methods 8, 665–670. https://doi.org/10.1038/nmeth.1635.

Yu, Y., Yang, J., Ejima, Y., Fukuyama, H., Wu, J., 2018. Asymmetric functional connectivity of the contra- and ipsilateral secondary somatosensory cortex during tactile object recognition. Front. Hum. Neurosci. 11, 662. https://doi.org/10.3389/FNHUM.2017.00662/BIBTEX.

Zhu, Z., Disbrow, E.A., Zumer, J.M., Mcgonigle, D.J., Nagarajan, S.S., 2007. Spatiotemporal integration of tactile information in human somatosensory cortex 14, 1–14. https://doi.org/10.1186/1471-2202-8-21.